

LOCAL CHARACTERIZATION OF CO-FIRING-INDUCED INHOMOGENEITIES OF CONVENTIONAL MC-SI SOLAR CELLS

A. Schütt, J. Carstensen, J.-M. Wagner, and H. Föll

Institute for Materials Science, Faculty of Engineering, Christian-Albrechts-University of Kiel, Kaiserstr. 2, 24143 Kiel, Germany, email: jc@tf.uni-kiel.de, Phone: (+49) 431 880 6181, Fax: (+49) 431 880 6178

ABSTRACT: All modifications of the cell process, e.g. changing the front or rear pastes or the sheet resistance, usually need a time and money consuming adaptation of the co-firing process (typically belt speed and T_p) or even a readjusting of the whole cell process, because statistically relevant improvements of the efficiency are used for the optimization procedure. In this paper CELLO measurements are used to generate local maps of the bulk life-time τ_{life} , the surface recombination velocity at the back side S_B , and the series resistance R_{ser} . A systematic co-firing optimization with various co-firing conditions using around 40 multicrystalline cells from neighboring wafers has been monitored by more than 1500 CELLO maps. The results and strategies for an efficient process optimization are discussed.

Keywords: Characterization, manufacturing and processing, metallization, multicrystalline silicon

1 INTRODUCTION

Efficient solar cell production requires a co-firing process, i.e. the simultaneous formation of the front grid contact and the Al back contact using a sophisticated temperature profile. The co-firing process parameters like choice of the paste, belt speed of the furnace (which determines the heating time), and the temperature profile (characterized especially by the peak temperature) do not only determine the quality of the obvious solar cell parameters like the ohmic front and rear contact, but also essential "secondary" effects like hydrogenation and gettering (which strongly influence bulk recombination) and the back surface field (BSF) formation (which determines the surface recombination velocity at the back side S_B). Due to the large number of co-firing process parameters and the large number of optimization parameters, the co-firing optimization is a time and money consuming process, which in an industrial environment requires a large number of produced solar cells in order to get statistically relevant information about the measured solar cell parameters. In this study CELLO measurements are used to generate maximal information about local solar cell properties to check if this allows a significant reduction of the number of solar cells produced to optimize the co-firing process. In this paper mainly the maps of S_B and of the series resistance R_{ser} are used to analyze their dependence on two co-firing process parameters: peak firing temperature T_p and belt speed.

2 THEORY

The temperature–time profile of the final co-firing step and thus the peak firing temperature T_p and the belt speed have tremendous impact on the multicrystalline Si solar cell properties:

- a) Sintering of the front contacts: The surface-near formation of Ag crystallites shows a dependence on the Si grain orientation and is synonymous with overfiring [1], it thus determines the front contact resistance. Additionally an inhomogeneous heat distribution of the furnace [1, 2] may induce patterns

of higher series resistance due to over- or underfiring. Overfiring may also lead to a deterioration of the p-n junction (worsening of the local diode parameters) or a shunting of the junction, which results in linear or non-linear shunts.

- b) Rear contact and BSF formation: A high peak temperature in combination with a medium to large thickness of the rear-side paste leads to an agglomeration of the liquid Al/Si in the form of islands with different BSF thicknesses underneath the islands [3] and thus inhomogeneous S_B .
- c) Hydrogenation and gettering: At around 840 °C hydrogen from the SiN layer is released that passivates defects in the bulk and thus improves the bulk life-time. Additionally, the bulk life-time may benefit from Al–P co-gettering during the co-firing process.

3 EXPERIMENTAL

3.1 Sample preparation and characterization

From neighboring multicrystalline p-Si wafers (125 cm × 125 cm, 300 μm thick) solar cells are produced by an industrial-like full-area Al BSF cell process that includes isotropic etching, inline diffusion (45 Ω/□ emitter), PECVD-SiN as antireflection coating, screen printing of front (PV 145) and rear pastes (PV 322), co-firing in IR belt furnace (5 zones, Centrotherm), and final edge insulation [4, 5].

For most of the process parameters optimal values found in previous runs have been chosen. Analyzing integral I – V curve data of a set of 160 solar cells, most fundamental parameters of the temperature profile were defined, indicating a possible range from 840 °C to 915 °C for the optimal peak temperature T_p (cf. Fig. 1). The integral I – V curve data suggested an optimal temperature–time product (with a large degree of uncertainty) around a peak temperature T_p of 870 °C and a belt speed of 1800 mm/min. Additionally a large variation of photo-current losses was observed, whose origin was not clear.

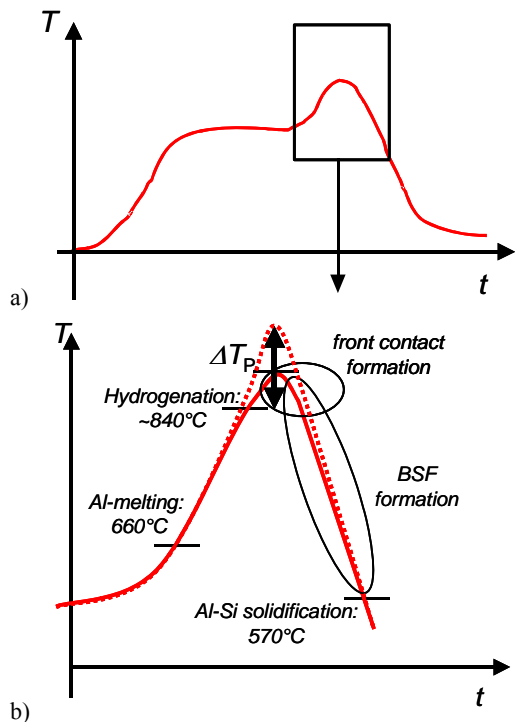


Fig. 1: a) Typical temperature–time profile of the co-firing step, b) zoom of the temperature peak with front- and rear side contact formation, hydrogenation, and BSF formation as parallel processes.

For the study in this paper more than 40 solar cells were produced with a systematic variation of the temperature–time product using

1. a fixed belt speed of 1800 mm/min and temperature variation between 840 °C and 915 °C,
2. a fixed temperature of 870 °C and variation of belt speed from 1800 mm/min down to 1500 mm/min,
3. a fixed temperature of 915 °C and variation of belt speed from 1800 mm/min up to 2100 mm/min.

Two cells each were fabricated for these three variation series to reduce the loss of information related to wafer breakage or outliers.

4 RESULTS AND DISCUSSION

In order to reduce the number of cells needed to get statistically relevant information about the efficiency dependence on the co-firing process, a three-step approach is used. Due to obvious cracks and outliers identified by integral I – V curve data the number of solar cells reduced to 30. These 30 cells are subject to fast CELLO series resistance and photocurrent measurements as discussed in [6]; this excluded 6 outliers, e.g. small cracks due to handling or variations that are not related to the varied parameters. For the remaining 24 cells a detailed impedance analysis [7, 8] was carried out which allows to calculate individual maps for e.g. bulk life-time, surface recombination at the back side, and series resistance data.

Figure 2 presents standard CELLO series resistance maps R_{ser} (right) and maps of the time constant $R_{ser}C$ extracted from for the impedance fit (left). The areas with

large series resistance show up in both sets of maps, which can serve as a consistency check for the impedance data. The solar cells analyzed in Fig. 2 have been produced with various T_p and a constant belt speed of 1800 mm/min. Some broken grid fingers are visible. The essential information about the optimal T_p is contained in the fraction of areas with drastically increased series resistance. Typical for overfired contacts are areas with increased series resistance reflecting certain grains (white marks), i.e. the defects formed in overfired cells are mostly material-related [1]. In contrast, underfiring is indicated by a pattern caused by furnace heat distribution (violet mark) [2]. The same area and pattern, sometimes even significantly larger than visible in Fig. 2b), is found in nearly all underfired cells. The best series resistance is found for 870 °C as already suggested by previous I – V curve measurements.

Similar results were obtained (not presented here) for a constant T_p at 870 °C and varying belt speed. Reducing the belt speed below 1700 mm/min, i.e. increasing the time within the furnace, the ohmic front contact resistance slightly reduced, but the local diode quality, especially in areas with high dislocation density, became significantly worse.

While for the series resistance at least some information about optimal firing temperature could be extracted from the integral data, allowing a consistency check of the CELLO results presented in this paper, this was not possible for the recombination losses. One main reason for this lies in the fact that for the integral values of the back surface recombination velocity S_B not even reliable measurements exist. So from the integral I – V curve data it could not be distinguished whether the strong variation in recombination losses were related to bulk (indirectly by changing the hydrogen passivation condition) or surface recombination at the back side (directly by the firing condition of the Al-BSF).

Figure 3 shows a selection of S_B maps for the series of constant belt speed (like in Fig. 2). Clearly the 840 °C map in Fig. 3a) has the lowest average value — around 600 cm/s (not considering the R_{ser} artifact marked by the violet line) — and is very homogeneous. In contrast all other maps have average values of around 900 cm/s and show a strong variation within the map. The maps of the bulk life-time (not shown here) were quite homogeneous with only a slight variation in the average value. So these results clearly indicate that the strong variation found from the I – V curve analysis are (only) related to different surface recombination velocities at the back side of the cell. Secondly, the optimal peak firing temperature with respect to S_B is around 840 °C, which is significantly below the optimal temperature of 870 °C for R_{ser} . At 840 °C the front contact is considerably underfired, leading to the R_{ser} artifact marked in the upper part of the map. Actually this area coincides with the area marked by the violet line in Fig. 2b) just rotating the map by 180° thus showing the typical fingerprint of the furnace for underfired cells (in this paper for an easy identification of material-induced defects all maps of neighboring cells have been oriented to show the corresponding grain structure).

The temperature dependence of S_B can be well understood by the so-called Al–Si agglomeration [3], i.e. inhomogeneous BSF thickness due to island growth that is typically observed for $T_p > 850$ °C when using thick rear Al pastes.

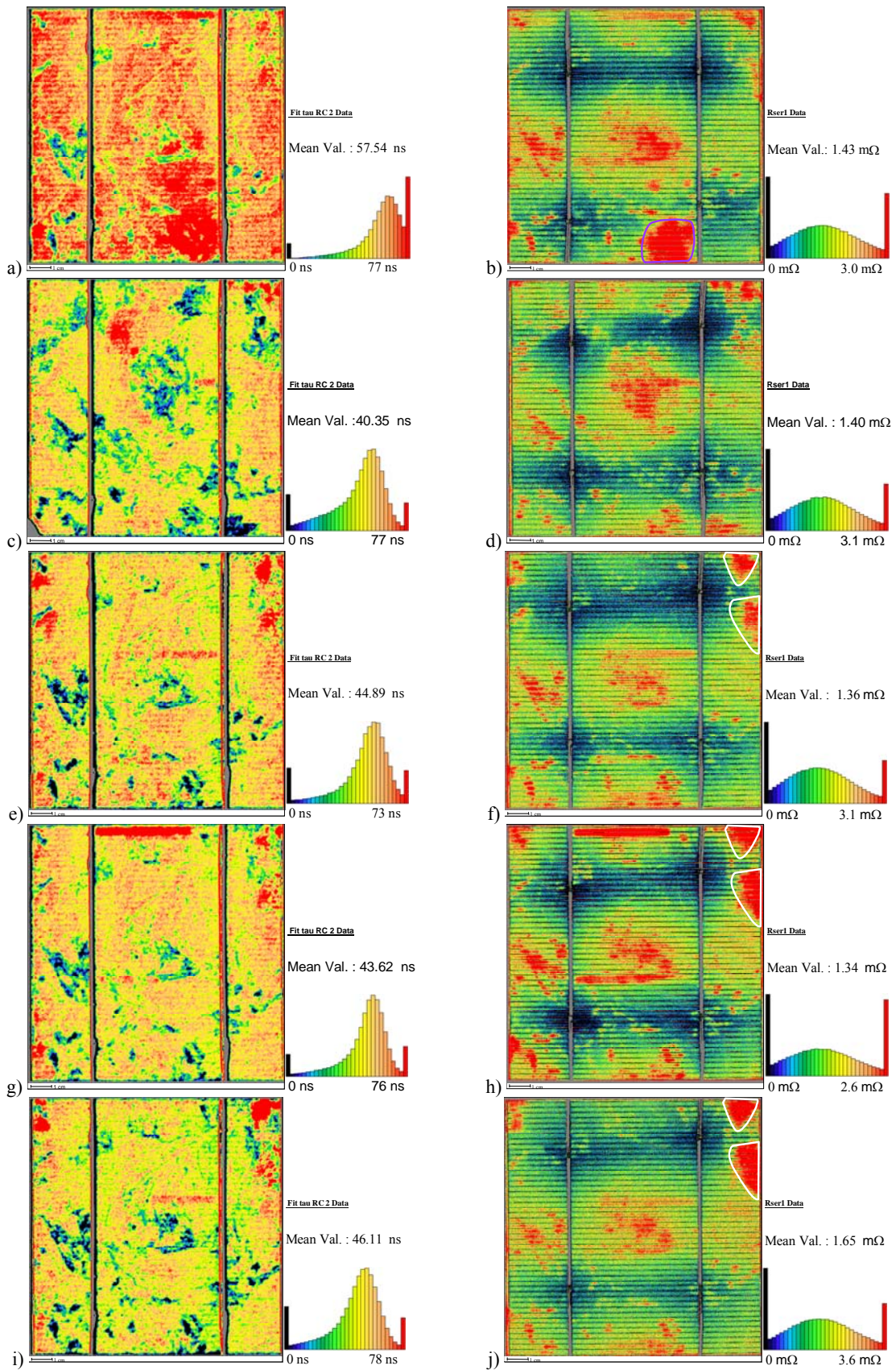


Fig 2: Fit to $R_{ser}C$ time constants (left) and conventional CELLO series resistance maps (right) for a fixed belt speed of 1800 mm/min and various T_p : a) and b) at 855 °C, c) and d) at 870 °C, e) and f) at 885 °C, g) and h) at 900 °C, and i) and j) at 915 °C. Typical underfired (violet) and overfired (white) areas are indicated.

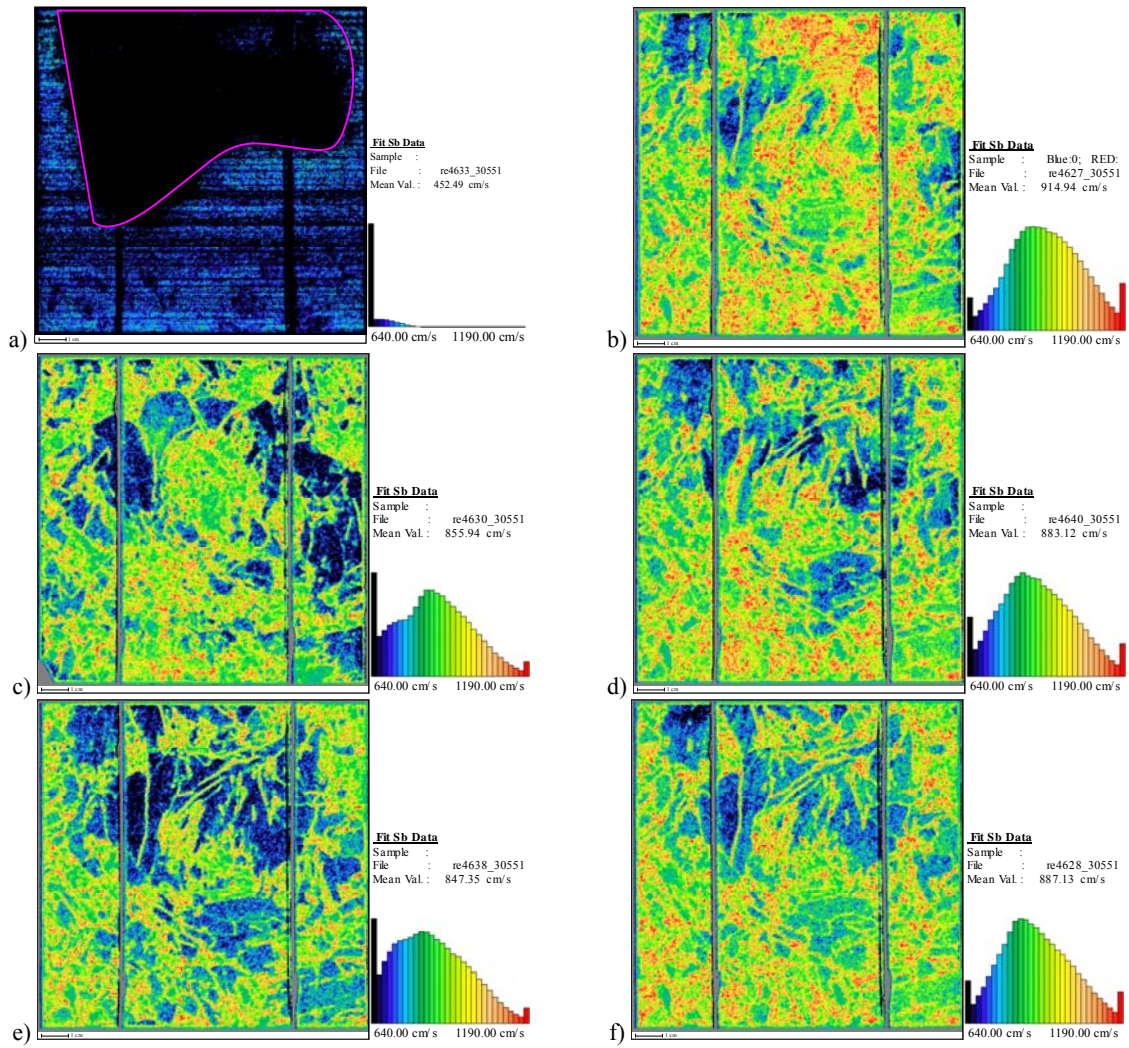


Fig. 3: S_B maps for a fixed belt speed of 1800 mm/min and various T_p : a) 840 °C, b) 855 °C, c) 870 °C, d) 885 °C, e) 900 °C, f) 915 °C.

Optimizing the cell process means to simultaneously optimize S_B and R_{ser} , i.e. to modify the firing condition in order to find the smallest average values and the smallest variation within the maps for S_B and R_{ser} for the same peak temperature T_p and belt speed. Probably the best strategy is to increase the critical temperature for Al-Si agglomeration by decreasing the printed Al rear paste thickness or by using an Al rear paste with a higher Si content, cf. [3] for details.

As this example shows, especially for mc-Si solar cells process optimization requires a local analysis of all relevant cell parameters because mainly the strong lateral variation of several efficiency-determining parameters is the main problem for mc-Si solar cells. Especially the series resistance of the front contact and the surface recombination induced by the back surface field strongly depend on the grain orientation. A "robust" co-firing process is needed which independently of the grain orientation allows for these two parameters to be optimal.

In addition the position, size, and shape of areas with e.g. very bad contact resistance allow a characterization of mechanisms leading to losses at non-optimal T_p . In the example presented in this paper underfired cells show areas with bad contact resistance which can clearly be

associated to the furnace (i.e. are process-related), while overfired cells show resistance losses at certain grains (i.e. are material-related). To identify such material-related effects the choice of neighboring wafers was essential.

5 CONCLUSION

This paper shows the clear advantage of using locally resolved data for solar cell process optimization in comparison to using only integral measurements like I - V curve data. Not only the mean values of the S_B and R_{ser} maps, but especially the deviation within the maps and the area fraction with "very bad" local properties allow a clear classification e.g. of the contact quality and the back surface field formation as a function of the co-firing parameters.

6 ACKNOWLEDGEMENTS

This work was supported by the Deutsche Forschungsgemeinschaft under grant No. FO 285/11-2.

7 REFERENCES

- [1] E. Cabrera, S. Olibet, J. Glatz-Reichenbach, R. Kopecek, D. Reinke, G. Schubert, *J. Appl. Phys.* **110**, 114511 (2011).
- [2] A.S.H. van der Heide, J.H. Bultman, J. Hoornstra, A. Schönecker, *Sol. Energy Mater. Sol. Cells* **74**, 43 (2002).
- [3] F. Huster, in *Proc. 20th European Photovoltaic Solar Energy Conference*, 1466, Barcelona (2005).
- [4] I. Cesar, E. Bende, G. Galbiati, L. Janßen, A. Weeber, J.H. Bultmann, in *Proceedings, 34th IEEE Photovoltaic Specialists Conference*, 1386, Philadelphia, USA (7-12 June 2009).
- [5] S. Keipert-Colberg, N. Barkmann, C. Streich, A. Schütt, D. Suwito, P. Schäfer, S. Müller, D. Borchert, in *Proc. 26th European Photovoltaic Solar Energy Conference*, 2BV.3.61, Hamburg (2011).
- [6] A. Schütt, J. Carstensen, H. Föll, S. Keipert-Colberg, D. Borchert, in *Proc. 26th European Photovoltaic Solar Energy Conference*, 2BV.2.39, Hamburg (2011).
- [7] J. Carstensen, A. Schütt, H. Föll, in *Proc. 24th European Photovoltaic Solar Energy Conference*, 1AO.4.5, Hamburg (2009).
- [8] A. Schütt, J. Carstensen, G. Popkirov, H. Föll, in *Proc. 26th European Photovoltaic Solar Energy Conference*, 2DO.3.3, Hamburg (2011).